Communication in Physical Sciences, 2021, 7(4): 278-288

First Principles Calculations of Structural, Electronic and Optical Properties of Nitrogen-Doped Titanium Dioxide for Solar Cells Application

Buhari Aminu Balesa, Abdullahi Lawal, Saddiq Abubakar Dalhatu ,Bala Idris and Mustapha Bello

Received: 24 September 2021/Accepted 29 November 2021/Published online: 15 November 2021

Abstract: *The dire requirement for less toxic, eco-friendly, cheaper, cost-effective and efficient material for solar cell application has led to increasing focus on a range of different source materials. In particular, the larger energy bandgap in TiO_2 has limited its application for solar cell applications. However, doping TiO_2 with non-metal such as N gives a broader absorption at the visible region and subsequently adjusts the bandgap, which allows better utilization of the solar spectrum. However, to exploit its potentials, a detailed analysis of structural, electronic and optical properties of N doped TiO_2 is necessary. In this work, first-principles calculations within the density functional theory (DFT) are carried out as an approach to address the problem. The calculated bandgap energy for pure TiO_2 (2.30 eV) was in strong agreement with the experimental value. The substitution of nitrogen (N) atom in the TiO_2 at the oxygen (O) and titanium (Ti) sites led to the reduction in the energy gap and the observation was also in good agreement with results from previous works. Our findings confirmed that non-metal doping narrows the energy band gap of semiconductor materials. The optical gap of 1.63 and 0.32 eV for N doped TiO_2 at oxygen (O) and titanium (Ti) sites, which indicated that N-dopedTiO_2 can be used to detect light in the near infrared and visible light regions. Direct energy gap, narrowing effects and strong light absorption of N-doped TiO_2 in the near infrared to visible light region suggest that the investigated material is most likely suitable for solar cells and near infrared optoelectronic applications.*

Keywords: *TiO_2, DFT, doping, nitrogen, solar cell.*

Buhari Aminu Balesa*
Department of Physics, Faculty of Science, Bauchi State University Gadau, Bauchi State Nigeria
Email: baminubalesa@gmail.com

Abdullahi Lawal
Department of Physics, Federal College of Education Zaria, P.M.B 1041, Zaria, Kaduna State Nigeria
Email: abdullahikubau@yahoo.com
Orcid id: 0000-0003-1294-3180

Saddiq Abubakar Dalhatu
Department of Physics, Faculty of Science, Bauchi State University Gadau, Bauchi State Nigeria
Email: sadgambaki@yahoo.com

Bala Idris
Department of Physics, Faculty of Science, Bauchi State University Gadau, Bauchi State Nigeria
Email: balaidris22@gmail.com

Mustapha Bello
Department of Physics, Faculty of Science, Bauchi State University Gadau, Bauchi State Nigeria
Email: mustaphabelloazare@gmail.com

1.0 Introduction

Several investigations on properties, behaviour and applications of transitional metal oxides have been carried out to create satisfaction for the increasing and demanding needs of

communities and industries (Maduraiveeran *et al.*, 2019, Han *et al.*, 2020). The main demand of the industry is to find economical alter environmentally which should be non-toxic, environmentally friendly, easily accessible and efficient (Dixit, 2012, Dash *et al.*, 2018). Consequently, numerous experimental and theoretical investigations are ongoing, in a search for better alternatives for the existing ones. Titanium dioxide (TiO_2) is one of the essential transition metal oxide semiconductors that has given a significant boost to several industries, including the green energy industries. Numerous properties of TiO_2 have been explored towards the achievement of its applications, notably, its high optical transmittance, strong absorbance of the visible and ultraviolet lights, low electrical resistivity, high ionic semiconductor (Mikami *et al*., 2000). In addition, the characters that enable its applications in flat panel displays, sensor, pigment, catalyst and transparent optoelectronic devices have also encouraged further research on the applications of TiO_2 (Yang *et al*., 2014, Dixit, 2012, Wang *et al*., 2012, Hitosugi *et al.*, 2010, Wagemaker *et al.*, 2002) TiO_2 exists in several polymorphs of rutile, anatase, brookite, columbite, baddeleyite, cotunnite, pyrite and fluorite. Three of them exist naturally while others need to be engineered. Among these, the three naturally occurring polymorphs of rutile, anatase and brookite have been synthesized extensively due to their remarkable properties (Wang *et al*., 2012, Thilagam *et al*., 2011, Sai and Bang-Gui, 2012). Rutile structure possesses the highest stability (Jaćimović *et al*., 2010) compare to others, anatase (Beltran' *et al*., 2001). However, in solar cell technology, TiO_2 has limited applications due to its wider bandgap nature. To use TiO_2 for a solar cell application, its bandgap should be tuned to capture the maximum range of the solar spectrum. Currently, doping is one of the best options for the tunning and improvement of the optoelectronic properties of some materials suitable for applications as absorbing layer for solar cells (Cerdán-Pasarán *et al*., 2019, Jiang *et al*., 2019). Doping can significantly adjust the physical properties of materials (Cerdán-Pasarán *et al*., 2019). Consequently, TiO_2 is doped repeatedly with diverse transition elements and metals to enhance its optical absorption, magnetic properties, conductivity as well as tune its bandgap (Tseng *et al*., 2016, Li *et al*., 2019, Avram *et al*., 2021, Piątkowska *et al*., 2021). In comparison with metal doping, doping of non-metals is an effective approach for narrowing the band-gap of material and thus lowering the energy requires for the electronic transition from the HOMO to the LUMO (Reisner and Pradeep, 2014). Non-metal doping with an atom such as N can enhance the optical absorption, conductivity, magnetic and electronic properties of semiconductor materials (Duan *et al*., 2015, Asahi *et al*., 2001, Wang *et al*., 2019).

Given the expected benefits of doping TiO_2 with nitrogen, the present study is aimed at implementing a theoretical investigation of the effect of doping N on structural, electronic, and optical absorptions of TiO_2 semiconductors. This was accomplished by adopting a first-principles approach based on DFT implemented within the Quantum Espresso package. Different exchange-correlation functional of GGAs and LDA were employed as the manipulated variables in this study.

2.0 Computational Details

The calculations presented in this work were performed with two open-source simulation packages, Quantum Espresso (Giannozzi *et al.*, 2009) and Yambo (Marini *et al*., 2009) codes. Yambo simulation package interfaces with QE for excited-state calculations (which uses DFT results as its input) were also employed for the calculations. (Sangalli *et al*., 2019, Barhoumi and Said, 2020, Marsili *et al*., 2016, Lawal *et al*., 2018) Electronic structure and optical properties of pure and N doped TiO_2 calculations were performed based on the pseudopotential plane-wave method. For N doped TiO_2, one atom of oxygen and titanium atoms were replaced by an

atom of N for building the doped structures. Figs. 1(a)-(c) show the three models. Wu-Cohen's generalized gradient approximation (WC-GGA) (Perdew *et al*., 1996a) Perdew-Burke-Ernzerhof generalized gradient approximation (PBE-GGA) (Perdew *et al*., 1996b) and local density approximation (LDA) (Becke, 1988) exchange-correlation potential were used for lattice dynamics of pure and N doped TiO_2. Norm-conserving pseudopotentials were used in modeling interactions between ionic core potential and electrons of Ti, O and N atoms. The Brillouin zone integration was performed using Monkhorst-Pack grid (Monkhorst and Pack, 1976) of $11 \times 10 \times 11$ k-points grids for structural and band structure calculations for both undoped and doped systems. 70 Ry cut-off energy of the plane-wave basis set was used to expand the wave functions and 270 Ry for charge density. However, in the performance of optical properties calculations, the complex dielectric constant was first evaluated, and the other properties were expressed in terms of it. The complex dielectric constant ε is given by $\varepsilon(\omega) = \varepsilon_1(\omega) + i\varepsilon_2(\omega)$, where ε_1 and ε_2 are real and imaginary parts of dielectric constant respectively. This suggest that, the complex dielectric function is suitable for the description of the optical properties at microscopic level or quantum mechanical level. The expression for the complex imaginary part of dielectric function $\varepsilon_2(\omega)$ has been derived in equation 1.

$$\varepsilon_2(\omega) = \frac{2\pi e^2}{\Omega\varepsilon_0}|\langle\psi_k^c|\hat{u}\times\vec{r}|\psi_k^v\rangle|\delta\left(E_k^c - (E_k^v + E)\right) \quad (1)$$

3.0 Results and Discussions

3.1 Structural properties of TiO_2

TiO_2 naturally occurs in three structures, namely, rutile, anatase and brookite. In this work, the rutile crystal structure of TiO_2 was optimized using the Quantum Espresso package and the optimised structure was shown in Fig. 1. The optimization was carried out using different DFT functionals, including GGA-PBE, GGA-PBEsol, GGA-WC and LDA. By exploiting the Murnagahan'equation of state, the structural parameters of lattice parameters
are obtained. The results of the structural parameters are tabulated in Table 1. Generally, our calculated lattice parameters (a, b and c) are in good agreement with experimental work, with the difference only up to 3.0% and 2.8% respectively. Furthermore, the calculated lattice parameters with GGA-PBE were found to be closer to experimental results compared to GGA-PBEsol, GGA-WC and LDA.

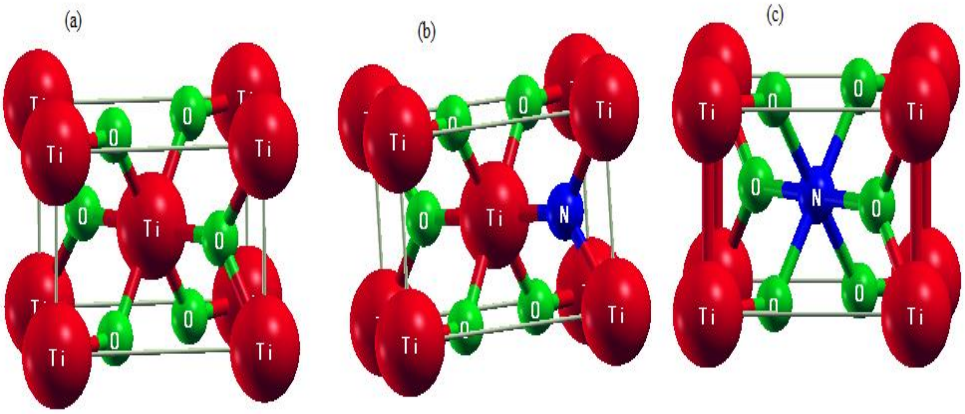

Fig. 1. Crystal structure of (a) Pure TiO_2 (b) N Doped TiO_2 at O (c) N doped TiO_2 at Ti site

Table 1: Calculated and experimental lattice constants of TiO_2

Ref.	XC	*a* (Å)	*b* (Å)	*c* (Å)
Present work	LDA	4.634	4.634	2.976
	PBE-GGA	4.543	4.543	2.961
	PBEsol	4.613	4.613	2.849
	GGA-WC	4.640	4.640	2.990
Experiment (Gerward and Olsen, 1997)		4.592	4.592	2.958

3.2. Electronic properties of pure TiO_2 and N Doped TiO_2

Electronic properties calculation is very important for describing the optoelectronic properties of semiconductor material. The electronic properties investigations of TiO_2 and N doped TiO_2 cover the electronic band structure, density of state (DOS) and partial density of state (PDOS). The main purpose of the ground state, electronic band structure, DOS and PDOS calculations in this work is to obtain Kohn Sham (KS) eigenvalue and eigenfunctions as well as useful information about the electronic properties of the concerned materials. The calculated electronic band structures of pure TiO_2 and N doped TiO_2 are displayed in Figure 2. The band structures of both pure and N doped TiO_2 were analyzed along with the special symmetry directions of the irreducible Brillouin zone along with the nine symmetries $\Gamma \rightarrow X \rightarrow \Delta \rightarrow P \rightarrow \Gamma \rightarrow T \rightarrow Y \rightarrow K \rightarrow H$ directions and the energy range of the band structure is plotted from 0.0 eV to 3.9 eV. The position of the Fermi level in the band structure of these crystals is shown by setting it to be zero on the energy scale. PBE exchange correlation potential is chosen over LDA, because in several cases GGA-PBE gives more reliable and accurate results for DFT electronic properties calculation. Band structures were calculated within PBE plus spin orbit coupling (SOC). For band structure calculations within PBE +SOC, the energy separation between the bottom of the conduction band and the top of the valence band occurred at the Γ, indicating that TiO_2 in the rutile phase has a direct bandgap with 2.30 eV energy gap, this value is close to experiment value of 3.0 eV when compared with other DFT calculations. Previous band structure calculations of pure TiO_2 in rutile phase within first-principles approach without taking into account the effect of SOC obtained a value of 1.88-2.10 eV [1-5]. The consistency of our result with experiment data is due to the effects of SOC. In order to investigate the effect of N-doping in TiO_2, calculations were performed for TiO_2 with N substitution. After N-doping at the oxygen site the conduction band edge [Figure 2(b)] shows a slight change in a position towards the lower energy and valence band towards the higher energy. The bandgap of single-atom nitrogen-doped TiO_2 at the oxygen site is reduced from 2.30 to 1.63 eV. It is well known that direct bandgap semiconductor material shows the optical activity of the material, which can be used for optoelectronic and solar cell applications. On the other hand, when the nitrogen atom replaced one atom of Ti atom, the bandgap reduced from 2.30 to 0.32 eV. It can be seen from Figure 2 (c) that the minimum of the conduction band changed from Γ to P point indicating its indirect nature of bandgap. This trend of reduction of bandgap value in single atom doping is in good agreement with the previous theoretical approaches (Butt *et al*., 2018, Lawal *et al*., 2021) and experiment measurement (Mushtaq *et al*., 2016). Our calculated bandgap values together with previous theoretical results and experimental data are given in Table 2.

To explore further on the electronic structure of undoped and N-doped TiO_2, we calculated the density of states (DOS) and partial density of states (PDOS) with DFT+SOC method. The density of states plays an important role in the formation of bands and the study of the bandgap. Results of DOS will assist in clearly understanding the nature of the bands while PDOS provides information about the atomic orbital contribution of the bands. The calculated DOS of undoped and N-doped TiO_2 are displayed in Figure 3. Figure 4 (a) depicts the PDOS of undoped TiO_2 per orbital type that is *s*-, *p*- and *d*-orbitals per Ti and *s*-, *p*- orbital for O atoms. The energetical valence bands which is situated between -1.5 eV to -6.3 eV is principally due to *s*- and *p*-orbitals of Ti and O atoms with a minor contribution of *d*-orbital of Ti atoms. On the other hand, the lowest of the conduction bands consists of *d*-orbitals of Ti atoms with little contribution from *s*- and *p*-orbitals of Ti and O atoms. PDOS of N-doped TiO_2 by substituting N atom at O sites are shown in Figure 4 (b). The maximum of the valence band near to the Fermi level comes from *p*-orbitals of Ti, *s*- and *p*-orbitals of O and N atoms. Conversely, the *s*-orbital of Ti atom is the main contributor of the lowest valence bands. The minimum conduction bands primarily come from the *p*-orbital of Ti atoms. Figure 4 (c) shows a result of PDOS of N-doped TiO_2 at one Ti site atom. Both valence bands majorly consist of *p*-orbitals of Ti atoms, *s*-orbital of O atoms and *p*-orbital of N atoms with a small contribution from *s*-orbital of Ti atom, *p*-orbitals of O atoms and *s*-orbital of N atoms in terms of hybridization. The conduction band (CB) is composed of *s*-orbital of Ti atoms, *p*-orbitals of O atoms and *s*-orbital of N atoms with little contribution from *p*-orbitals of Ti atoms, *s*-orbital of O atoms and *p*-orbital of N atoms.

Table 2: Results of band gap for TiO_2 polymorphs of rutile and N doped TiO_2. The results are compared with available experimental data and other first principles calculations

Polymorth	Work	Exchange Correlation Functional	Bandgap value, E_g(eV)	Type of bandgap
TiO2 (Rutile)	Present work	PBE-GGA+SOC	2.30	Direct (Γ - Γ)
	Previous work	Experiment(Reyes-Coronado *et al*., 2008)	3.00	-
		PBE-GGA(M Landmann *et al*., 2012)	1.88	Direct (Γ - Γ)
		PBE-GGA (Sai and Bang-Gui, 2012)	1.89	Direct (Γ - Γ)
		EV-GGA(Baizaee and N.Mousavi, 2009)	1.90	Direct (Γ - Γ)
		GGA (Xing-Gang *et al*., 2009)	1.91	Direct (Γ - Γ)
		PBE-GGA (Luciana Fernández-Werner *et al*., 2011)	2.10	Direct (Γ - Γ)
N doped TiO2 at O site	Present work	PBE-GGA+SOC	1.63	Direct (Γ - Γ)
N doped TiO2 at O site		PBE-GGA+SOC	0.32	Indirect

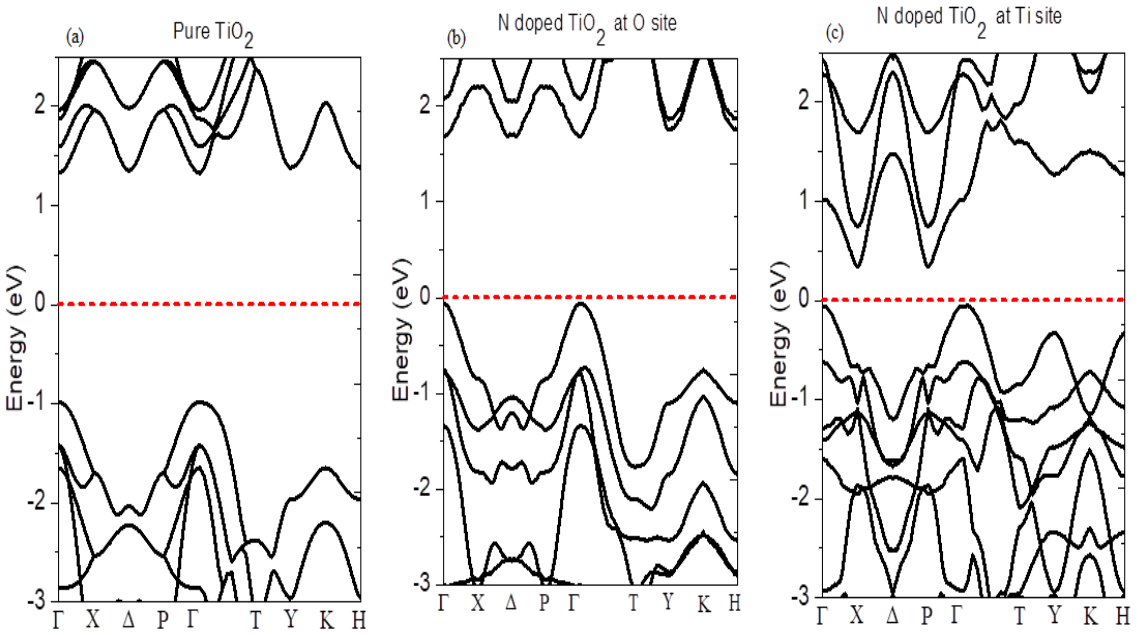

Fig. 2: Band structure of (a) Pure TiO_2 (b) N doped TiO_2 at O site and (c) N doped TiO_2 at Ti site

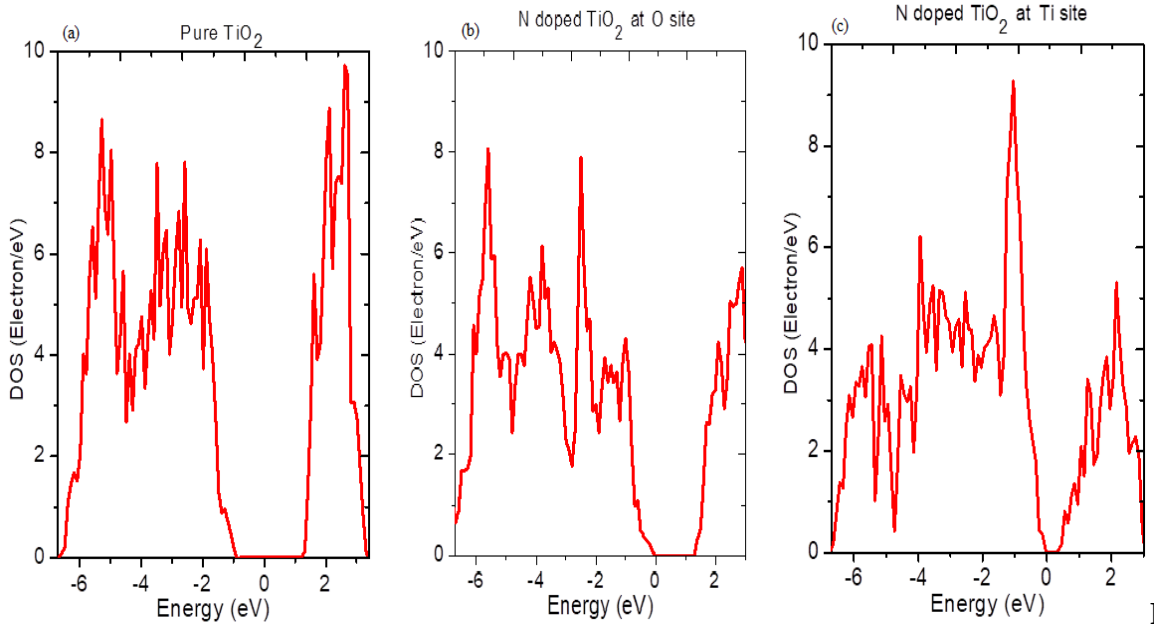

Fig. 3: Total density of states (DOS) of (a) pure TiO_2 (b) N doped TiO_2 at O site (c) N doped TiO_2 at Ti site

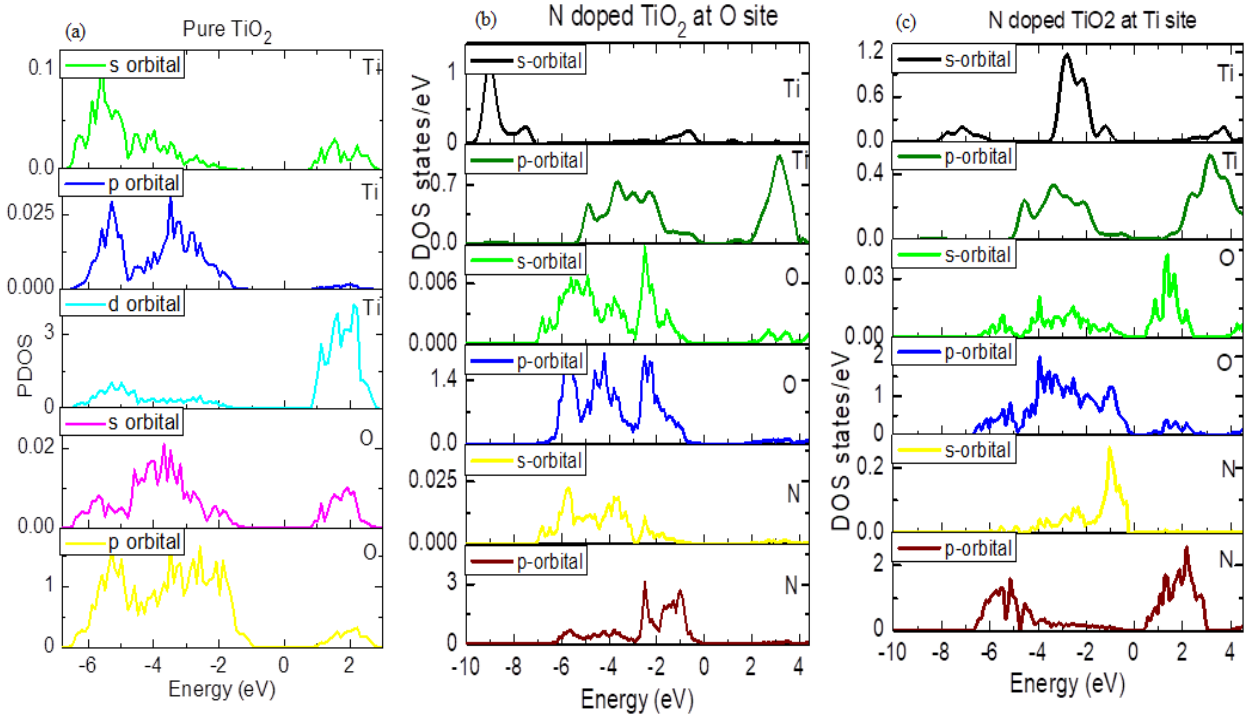

Fig. 4: Total density of states (DOS) of (a) Pure TiO_2 (b) N doped TiO_2 at O site (c) N doped TiO_2 at Ti site

.

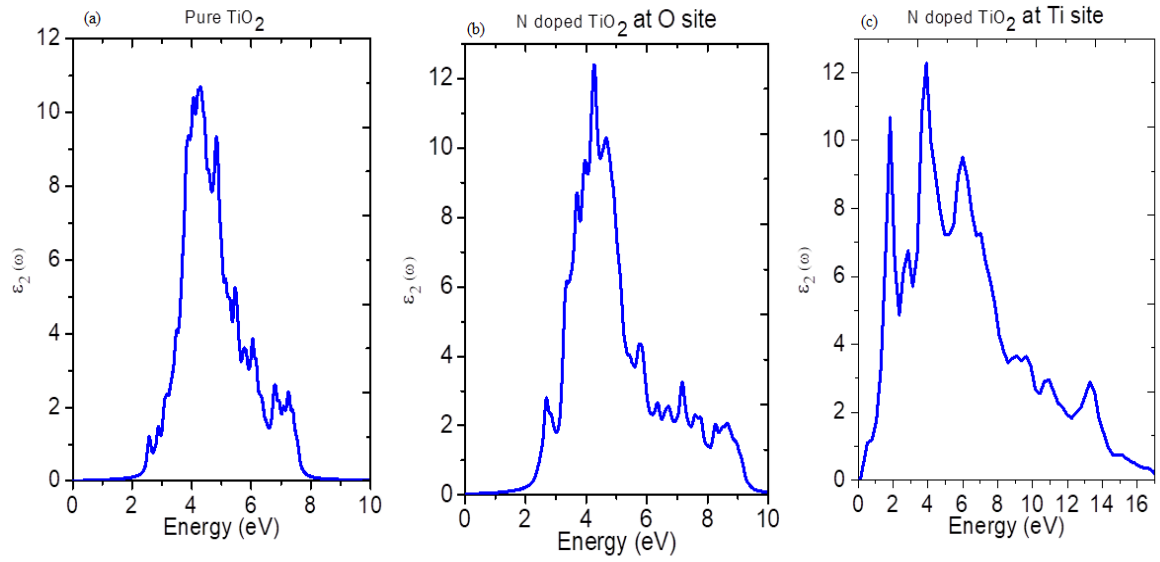

Fig. 5: The imaginary part of the frequency-dependent dielectric function of (a) Pure TiO_2 (b) N doped TiO_2 at O site and (c) N doped TiO_2 at Ti site

3.3. Optical Properties of Pure TiO_2 and N Doped TiO_2

The study of optical properties of a material is crucial to have an insight on its characteristics for the applications in optoelectronic systems and devices. Normally, optical properties describe the behavior of the material when exposed to electromagnetic emissions. From the literature, it was found that the exploration of the optical features relating to N-doped TiO_2 has not been done. The optical properties of pure TiO_2 and N doped TiO_2 are computed using

random phase approximation (RPA) based on PBE-GGA+SOC. The optical parameter considered in this paper is the imaginary part of the dielectric function $\varepsilon_2(\omega)$. The imaginary part $\varepsilon_2(\omega)$ of frequency dependent of the dielectric function relates to how light is absorbed by the medium (LAWAL, 2017, Lawal *et al*., 2017, Radzwan *et al*., 2020, Radzwan *et al*., 2018)The obtained imaginary part of frequency-dependent dielectric function of TiO_2, N doped TiO_2 at O site, and N doped TiO_2 at Ti site are displayed in Figure 5 (a), (b) and (c) respectively. For undoped TiO_2 crystal, the first critical point sometimes called the edge of optical absorption (optical gap) occurred at about 2.30 eV, this value corresponds to the fundamental bandgap. The calculated optical gap of undoped TiO_2 is in good agreement with experimental data. This point split the valence band maximum and conduction band minimum. For N doped TiO2 at O and Ti sites, the optical gap was found to be 1.63 and 0.32 eV. The optical gaps of 1.63 and 0.32 eV for N doped TiO2 at O site and Ti site, suggest that N doped TiO_2 is a promising candidate for solar cells and near infrared opto-electronic applications such as gas sensing and optical communication.

4.0 Conclusion

In this paper, optoelectronic properties of pure and N doped TiO_2 were investigated by using computational approaches within the framework of DFT. The calculations were carried out using Quantum Espresso and Yambo packages. To exploit the potential of the studied materials structural, electronic and optical properties were investigated. The generated structures of the studied materials were optimized. The results of the optimized structures concerning structural parameters were found to agree with the experimental results. The obtained bandgap energy for pure TiO_2 was found to 2.30 eV and this value is close to experimental results. Substituting N atom in the TiO2 at the O and Ti sites led to the reduction in the energy bandgap and this trend is in good agreement with previous work. Our findings confirmed that non-metal doping narrows the energy gap of semiconductor materials. The optical gap of 1.63 and 0.32 eV for N doped TiO_2 at O and Ti sites indicated that N-dopedTiO_2 can be used to detect light in the near infrared region and visible light wavelengths. Direct gap, narrowing effects and strong light absorption of N-doped TiO_2 in the near infrared to visible light region suggest that the investigated material is suitable for solar cells and near infrared optoelectronic applications.

5.0 References

Asahi, R., Morikawa, T., Ohwaki, T., Aoki, K. & Taga, Y. 2001. Visible-light photocatalysis in nitrogen-doped titanium oxides. *Science*, 293**,** pp. 269-271.

Avram, D., Patrascu, A. A., Istrate, M. C., Cojocaru, B. & Tiseanu, C. 2021. Lanthanide doped TiO2: Coexistence of discrete and continuous dopant distribution in anatase phase. *Journal of Alloys and Compounds*, 851**,**156849,https://doi.org/10.1016/j.jallcom.2020.156849

Baizaee, S. M. & N.Mousavi 2009. First-principles study of the electronic and optical properties of rutile TiO2. *Physica B*, 404**,** pp. 2111-2116.

Barhoumi, M. & Said, M. 2020. Correction of band-gap energy and dielectric function of BiOX bulk with GW and BSE. *Optik***,** 164631,https://doi.org/10.1016/j.ijleo.2020.164631.

Becke, A. D. 1988. Density-functional exchange-energy approximation with correct asymptotic behavior. *Physical Review A*, 38**,** 3098, https://doi.org/10.1103/PhysRevA.38.3098

Beltran', A., Sambrano, J. R., Sensato, M. C. R. & Andres', J. 2001. Static simulation of bulk and selected surfaces of anatase TiO_2. *Surface Science*, 490, 1, 2, pp. 116-124,.

Butt, F. K., Li, C., Haq, B. U., Tariq, Z. & Aleem, F. (2018). First-principles calculations of nitrogen-doped antimony triselenide: A prospective material for solar

cells and infrared optoelectronic devices. *Frontiers of Physics,* 13**,** 137805, https://doi.org /10.1007/s11467-018-0790-2.

Cerdán-Pasarán,A., López-Luke, T., Mathew, X. & Mathews, N. R. 2019. Effect of cobalt doping on the device properties of Sb2S3-sensitized TiO_2 solar cells. *Solar Energy,* 183**,** pp. 697-703.

Dash, D., Pandey, C. K., Chaudhury, S. & Tripathy, S. K. 2018. Structural, electronic, and mechanical properties of cubic TiO2: A first-principles study. *Chinese Physics B,* 27**,** 017102,https://doi.org/10.1088/16741056/27/1/017102 .

Dixit, H. 2012. *First-principles electronic structure calculations of transparent conducting oxide materials.* PhD, Universiteit Antwerpen.

Duan, T., Liao, C., Chen, T., Yu, N., Liu, Y., Yin, H., Xiong, Z.-J. & Zhu, M.-Q. 2015. Single crystalline nitrogen-doped InP nanowires for low-voltage field-effect transistors and photodetectors on rigid silicon and flexible mica substrates. *Nano Energy,* 15**,** pp. 293-302.

Gerward, L. & Olsen, J. S. 1997. Post-Rutile High-Pressure Phases in TiO_2. *Journal of Applied Crystallography.,* 30,3, pp. 259-264.

Giannozzi, P., Baroni, S., Bonini, N., Calandra, M., Car, R., Cavazzoni, C., Ceresoli, D., Chiarotti, G. L., Cococcioni, M. & Dabo, I. 2009. QUANTUM ESPRESSO: a modular and open-source software project for quantum simulations of materials. *Journal of physics: Condensed matter,* 21**,** 395502, https://doi.org/10.1088/09538984/21/39/395502

Han, Z., Qi, Y., Yang, Z., Han, H., Jiang, Y., Du, W., Zhang, X., Zhang, J., Dai, Z. & Wu, L. 2020. Recent advances and perspectives on constructing metal oxide semiconductor gas sensing materials for efficient formaldehyde detection. *Journal of Materials Chemistry C,* 8**,** pp. 13169-13188.

Hitosugi, T., Yamada, N., Nakao, S., Hirose, Y. & Hasegawa, T. 2010. Properties of TiO2-based transparent conducting oxides. *Phys. Status Solidi A,* 207**,** pp. 1529-1537.

Jaćimović, J., Vâju, C., Gaál, R., Magrez, A., Berger, H. & Forró, L. 2010. High-Pressure Study of Anatase TiO2. *Materials,* 3,3, pp.1509-1514.

Jiang, C., Tang, R., Wang, X., Ju, H., Chen, G. & Chen, T. 2019. Alkali Metals Doping for High-Performance Planar Heterojunction Sb2S3 Solar Cells. *Solar RRL,* 3**,** 1800272, https://doi.org/10.1002/solr.201800272.

Lawal, A. 2017. Theoretical study of structural, electronic and optical properties of bismuth-selenide, bismuth-telluride and antimony-telluride/graphene Heterostructure for Broadband Photodetector. Universiti TeknologiMalaysia,http://eprints.utm.my/id/eprint/79206/1/AbdullahiLawalPFS2017.pdf

Lawal, A., Shaari, A., Ahmed, R. & Jarkoni, N. 2017. First-principles many-body comparative study of Bi2Se3 crystal: A promising candidate for broadband photodetector. *Physics Letters A,* 381**,** pp. 2993-2999.

Lawal, A., Shaari, A., Ahmed, R. & Taura, L. 2018. Investigation of excitonic states effects on optoelectronic properties of Sb2Se3 crystal for broadband photo-detector by highly accurate first-principles approach. *Current Applied Physics,* 18**,** pp. 567-575.

Lawal, A., Shaari, A., Taura, L., Radzwan, A., Idris, M. & Madugu, M. 2021. G0W0 plus BSE calculations of quasiparticle band structure and optical properties of nitrogen-doped antimony trisulfide for near infrared optoelectronic and solar cells application. *Materials Science in Semiconductor Processing,*124**,**105592,https://doi.org/10.1016/j.mssp.2020.105592 .

Li, S., Yang, Y., Su, Q., Liu, X., Zhao, H., Zhao, Z., Li, J. & Jin, C. 2019. Synthesis and photocatalytic activity of transition metal and rare earth element co-doped TiO2 nano particles. *Materials Letters,* 252**,** pp**.** 123-125.

Luciana Fernández-Werner, Ricardo Faccio, Helena Pardo & Mombrú, Á. W. 2011. Electronic structure study of TiO2 polymorphs, evaluation of formic acid adsorption on dry (001) and (100) TiO2(B) facets by DFT calculations. *Nanotechnology*, https://arxiv.org/abs/1108.2721.

M Landmann, Rauls, E. & Schmidt, W. G. 2012. The electronic structure and optical response of rutile, anatase and brookite TiO2. *J. Phys. Condens.Matter*,24,19,195503,https://doi.org/10.1088/0953-8984/24/19/195503.

Maduraiveeran, G., Sasidharan, M. & Jin, W. 2019. Earth-abundant transition metal and metal oxide nanomaterials: Synthesis and electrochemical applications. *Progress in Materials Science*, 106**,** pp. 100574.

Marini, A., Hogan, C., Grüning, M. & Varsano, D. 2009. Yambo: an ab initio tool for excited state calculations. *Computer Physics Communications*, 180**,** pp. 1392-1403.

Marsili, M., Mosconi, E., De Angelis, F. & Umari, P. 2016. Large scale GW-BSE calculations with N3 scaling: excitonic effects in dye sensitised solar cells. *Physical ReviewB*,95,7,075415,https://doi.org/10.1103/PhysRevB.95.075415.

Mikami, M., Nakamura, S., Kitao, O., Arakawa, H. & Gonze, X. 2000. First-Principles Study of Titanium Dioxide: Rutile and Anatase. *Japanese Journal of Applied Physics*, 39(8B),L847,https://doi.org/10.1143/JJAP.39.L847.

Monkhorst, H. J. & Pack, J. D. 1976. Special points for Brillouin-zone integrations. *PhysicalreviewB*,13**,**5188,https://doi.org/10.1103/PhysRevB.13.5188.

Mushtaq, S., Ismail, B., Raheel, M. & Zeb, A. 2016. Nickel antimony sulphide thin films for solar cell application: study of optical constants. *Natural Science*, 8**,** pp. 33-40.

Perdew, J. P., Burke, K. & Ernzerhof, M. 1996a. Generalized gradient approximation made simple. *Physical review letters*, 77**,** 3865, https://doi.org/10.1103/PhysRevLett.77.3865.

Perdew, J. P., Burke, K. & Wang, Y. 1996b. Generalized gradient approximation for the exchange-correlation hole of a many-electron system. *Physical Review B*, 54**,** 16533, https://doi.org/10.1103/PhysRevB.54.16533.

Piątkowska, A., Janus, M., Szymański, K. & Mozia, S. 2021. C-, N-and S-Doped TiO2 Photocatalysts: A Review. *Catalysts*, 11**,** 144, https://doi.org/10.3390/catal11010144.

Radzwan, A., Ahmed, R., Shaari, A., Ng, Y. X. & Lawal, A. 2018. First-principles calculations of the stibnite at the level of modified Becke–Johnson exchange potential. *Chinese Journal of Physics*, 56**,** pp. 1331-1344.

Radzwan, A., Lawal, A., Shaari, A., Chiromawa, I. M., Ahams, S. T. & Ahmed, R. 2020. First-principles calculations of structural, electronic, and optical properties for Ni-doped Sb2S3. *Computational CondensedMatter*,24**,**e00477,https://doi.org/10.1016/j.cocom.2020.e00477.

Reisner, D. E. & Pradeep, T. 2014. *Aquananotechnology: global prospects*, CRCPress,https://books.google.com.ng/books?hl=en&lr=&id=UpstaU6fAJwC&oi.

Reyes-Coronado, D., Rodriguez-Gattorno, G., Espinosa-Pesqueira, M. E., Cab, C., Coss, R. D. & Oskam, G. 2008. Phase-pure TiO2 nanoparticles: anatase, brookite and rutile. *Nanotechnology*,19,14,145605,https://doi.org/10.1088/0957-4484/19/14/145605.

Sai, G. & Bang-Gui, L. 2012. Electronic structures and optical properties of TiO2: Improveddensity-functional-theory investigation*. *Chin. Phys. B*, 21(5), 057104, https://doi.org/10.1088/16741056/21/5/057104.

Sangalli, D., Ferretti, A., Miranda, H., Attaccalite, C., Marri, I., Cannuccia, E., Melo, P., Marsili, M., Paleari, F. & Marrazzo, A. 2019. Many-body perturbation theory calculations using the yambo code. *J. Phys.: Condens.Matter*,31,32,325902,https://doi.org/10.1088/1361-648X/ab15d0.

Thilagam, A., Simpson, D. J. & Gerson, A. R. 2011. A first-principles study of the dielectric properties of TiO2 polymorphs. *J. Phys.: Condens.Matter*,23,2,025901,https://doi.org/10.1088/0953-8984/23/2/025901.

Tseng, L.-T., Luo, X., Bao, N., Ding, J., Li, S. & Yi, J. 2016. Structures and properties of transition-metal-doped TiO2 nanorods. *Materials Letters,* 170**,** pp. 142-146.

Wagemaker, M., Kentgens, A. P. M. & Mulder, F. M. 2002. Equilibrium lithium transport between nanocrystalline phases in intercalated TiO2 anatase. *Nature Materials,* 418, 6896, pp. 397-399.

Wang, S., Fang, Y., Wang, X. & Lou, X. W. 2019. Hierarchical Microboxes Constructed by SnS Nanoplates Coated with Nitrogen-Doped Carbon for Efficient Sodium Storage. *Angewandte Chemie,* 131**,** pp. 770-773.

Wang, Z., Sun, R., Chen, C., Saito, M., Tsukimoto, S. & Ikuhara, Y. 2012. Structural and electronic impact of SrTiO3 substrate on TiO2 thin films. *J Mater Sci,* 47,13, pp. 5148-5157.

Xing-Gang, H., An-Dong, L., Mei-Dong, H., Bin, L. & Xiao-Ling, W. 2009. First-Principles Band Calculations on Electronic Structures of Ag-Doped Rutile and Anatase TiO2. *Chin. Phys. Lett.,* 26,7,077106, https://doi.org/10.1088/0256-307X/26/7/077106.

Yang, C.-T., Balakrishnan, N., Bhethanabotla, V. R. & Joseph, B. 2014. Interplay between Subnanometer Ag and Pt Clusters and Anatase TiO2 (101) Surface: Implications for Catalysis and Photocatalysis. *J Physical Chemistry C,* 118**,** pp. 4702-4714.

Conflict of Interest

The authors declared no conflict of interest. This work was carried out in collaboration among all authors. All authors read and approved the final manuscript

.